22-GHz Modulation Bandwidth of Long Cavity DBR Laser by Using a Weakly Laterally Coupled Grating Fabricated by Focused Ion Beam Lithography

L. Bach, W. Kaiser, J. P. Reithmaier, *Member, IEEE*, A. Forchel, M. Gioannini, V. Feies, and I. Montrosset

***Abstract*—A 22-GHz directly modulated 3-dB bandwidth could be obtained by 1.3-mm-long weakly laterally coupled distributed Bragg reflector lasers fabricated by focused ion beam lithography. In addition to a high bandwidth, the lasers show a stable emission spectrum with side-mode suppression ratios of more than 40 dB and output powers exceeding 20 mW.**

***Index Terms*—Distributed Bragg reflector (DBR) lasers, ion beam lithography, monolithic integration, optical communication, wavelength-division-multiplexing source.**

I. Introduction

DUE TO THE demand of a continuous increase of the transmission rates in all network levels, low-cost directly modulated lasers with high modulation bandwidths and single-mode emission are necessary. At the same time, the total laser performance shall not degrade under the optimization of the high-frequency characteristics. Theoretical [1]–[4], as well as practical [5], investigations have shown that specially designed distributed Bragg reflector (DBR) lasers can fulfill these demands. In conventional high-speed laser devices, the response time is mainly limited by the coupling between electronic states, i.e., interband transition, and the propagating electromagnetic field. In addition to this electron–photon resonance (EPR), there are also higher order resonances like the photon–photon resonance (PPR), which is caused by the revolution of a photon within the cavity [1], [2]. In conventional high-speed short cavity lasers, the PPR has no impact on the high-frequency response characteristics because the frequency distance between the two resonances is too large to get a coupling between EPR and PPR.

In this work, we have investigated long cavity DBR lasers with uncoated cleaved facets, which allow the coupling of the PPR by using weakly coupled DBR gratings fabricated by focused ion beam (FIB) lithography. With this type of laser, a large modulation bandwidth of 22 GHz, i.e., 2.5 times larger compared to Fabry–Pérot lasers, could be obtained for a 1.3-mm-long device in combination with stable emission properties, like high side-mode suppression ratio (SMSR) and high single-mode output power.

Manuscript received April 30, 2003; revised September 8, 2003. This work was supported by the European IST Project "Big Band" (IST-2001-34813) and by the State of Bavaria.

L. Bach, W. Kaiser, J. P. Reithmaier, and A. Forchel are with the Technische Physik, Universität Würzburg, D-97074 Würzburg, Germany (e-mail: LarsBach@gmx.de).

M. Gioannini, V. Feies, and I. Montrosset are with the Dipartimento di Elettronica Politecnico di Torino, LARCSO, I-10129 Torino, Italy.

Digital Object Identifier 10.1109/LPT.2003.820463

II. Design and Fabrication

As basic material, an eight quantum-well (QW) InGaAsP–InP laser structure was used, which was grown by gas-source molecular beam epitaxy. The active region consists of eight 6-nm-thick compressively strained InGaAsP QWs, which are separated by 10-nm-thick barriers. The gain maximum of this laser is located at 1550 nm at room temperature. The ridge waveguide (RWG) definition is realized by a selective dry–wet chemical etch process, which allows a well-defined RWG fabrication with vertical sidewalls and a smooth surface.

After the completion of the RWG, the grating is defined by FIB implantation of Ga^+ ions lateral to the RWG. The implantation creates a band gap shift at the implanted regions after a rapid thermal annealing step at 700 °C. This causes a periodic modulation of the band gap at the implanted parts of the grating of $\Delta E_{\rm gap} = 40$ meV. In addition to the band gap shift, the implantation generates a change of the crystal quality of the InP layer between the two etch stop layers in the implanted regions. This change results in a strongly increased etch rate for the implanted regions when using a 10% high-frequency solution [6]. This characteristic allows the fabrication of an additionally self-aligned index grating. The use of this grating fabrication enables the creation of complex coupled grating structures without any epitaxial overgrowth step. The sample was planarized by bisbenzocyclobutene, which serves as an insulator and the p-contact layers were evaporated. More details on the grating fabrication technology and device characteristics can be found elsewhere [7], [8].

III. Basic Device Properties

The lasers can be operated in continuous wave (CW) up to 90 °C in single mode. Fig. 1 shows the power–current (P–I) curves of a 1.3-mm-long DBR laser with a gain section length of 1000 μm and an unpumped grating section length of 300 μm for different operating temperatures between 10 °C and 90 °C. At 10 °C, a threshold current of 70 mA is measured, which increases to 110 mA at 70 °C for unmounted devices. A maximum output power of 25 mW could be obtained at 10 °C and 2 mW at 80 °C, respectively.

The lasers exhibit a high side-mode suppression value of more than 40 dB over the whole operation range. The laser, whose P–I characteristics are shown in Fig. 1, has a grating period of $\Lambda = 244$ nm and emits at room temperature at a wavelength of 1562 nm. From the analysis of subthreshold spectra [9], an index coupling coefficient of $\kappa_i = 34$ cm^{-1} has been determined. It turned out that the complex part of

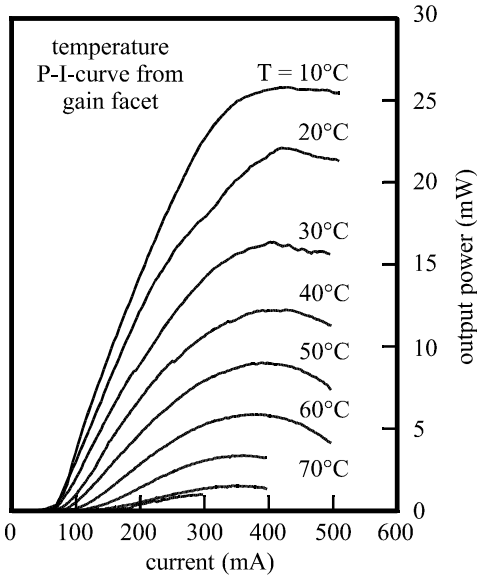

Fig. 1. P–I curves of the $1000 + 300$ μm DBR laser for different operation temperatures between 10 °C and 90 °C.

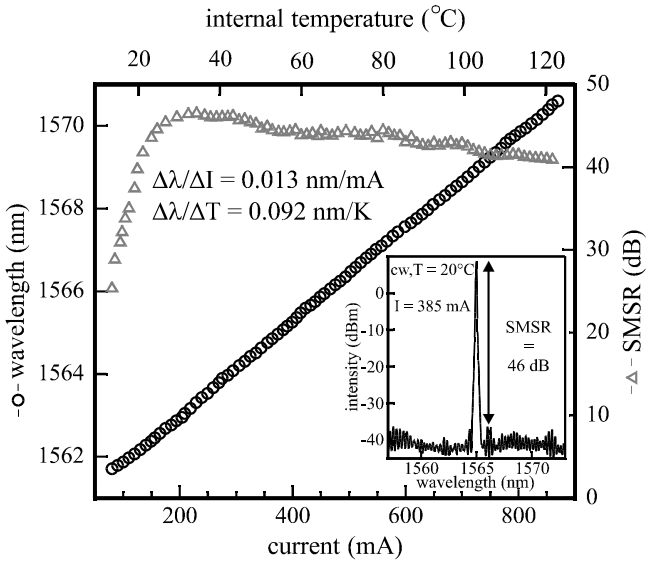

Fig. 2. Emission behavior of the DBR laser over the entire operation range between 100 and 900 mA. The triangles show the SMSR of the laser. The inset shows the emission spectrum of the laser at 385-mA drive current with an SMSR of 46 dB.

the coupling coefficient in such unpumped DBR gratings is negligible. In Fig. 2, the emission wavelength and SMSR is plotted as function of the operation current between threshold and more than 12 times the threshold current. Due to internal heating of the unmounted device, the wavelength is continuously tuned over 9 nm by the injection current. The internal temperature was evaluated from the wavelength shift using the temperature coefficient determined by temperature dependent pulsed measurements. The inset shows a single-mode spectrum with an SMSR of 46 dB at an operation current of 385 mA.

IV. High-Frequency Results and Discussion

The high-frequency modulation properties of DBR lasers, as well as of Fabry–Pérot lasers, for reference were characterized

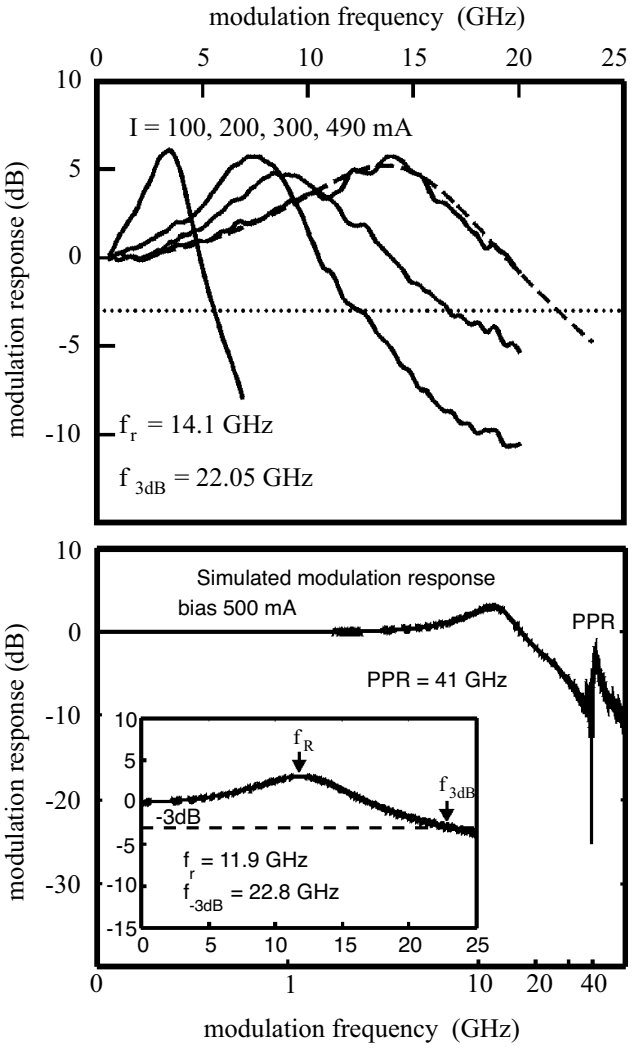

Fig. 3. Measured SSRF of the DBR laser for different bias currents (top). The dashed curve is a fit of a simulated resonance curve to the measured data to extrapolate the 3-dB bandwidth. Simulated response function at a bias current of 500 mA as function of modulation frequency on a logarithmic (bottom) and linear scale (bottom, inset).

by an optical network analyzer (HP 8703) with a bandwidth of 20 GHz for small signal modulation and by an optical signal analyzer (HP 70 000) with a bandwidth of 22 GHz for relative intensity noise (RIN) measurements, respectively.

Devices with different cavity lengths were investigated. The maximum 3-dB bandwidth of Fabry–Pérot lasers decreases continuously with increasing cavity length from 19.5 GHz at 0.5 mm down to 8 GHz at 1.6 mm. In comparison to these results, the DBR lasers behave differently. In general, higher modulation frequencies were obtained with longer devices. In Fig. 3 (top), small signal modulation results of the above-presented 1.3-mm-long device are shown. At an injection current of 490 mA, a maximum 3-dB bandwidth of 22 GHz can be determined by extrapolating the fitted resonance curve (dashed line). This value is about 2.5 times higher than for Fabry–Pérot lasers with the same cavity length and processed on the same wafer. We think that this strong increase is mainly caused by the coupling of the EPR with the PPR.

To get evidence, the small signal response function (SSRF) was simulated by taking into account the basic device proper-

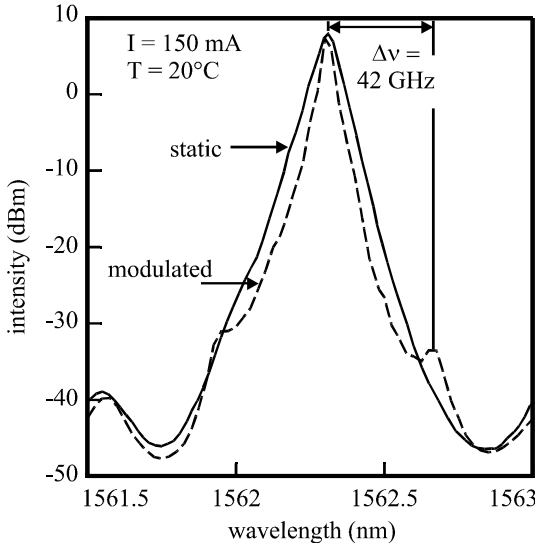

Fig. 4. Comparison between static and modulated operation regime (20 GHz) at a drive current of 150 mA. The modes spacing of 42 GHz corresponds to the PPR for this laser device.

ties, like gain, wavelength dependence, coupling strength of the DBR grating, etc., which were evaluated from current dependent subthreshold spectra. The measured results were fitted in order to extract the main cavity parameters [9]. The same spectra have also been obtained using a time-domain traveling-wave laser model [10] to set properly the parameters of the dynamic simulator. In Fig. 3 (bottom), the calculated SSRF is plotted in double logarithmic scale for an injection current of 500 mA. One can clearly identify a first resonance peak at 12 GHz and an additional resonance at 41 GHz. This resonance position is in agreement with a PPR expected for a 1.3-mm-long cavity. Due to the coupling of PPR with the main EPR, the damping for higher frequencies is strongly reduced. In the linear frequency plot [c.f., inset of Fig. 3 (bottom)], a 3-dB bandwidth of 22.8 GHz can be determined in excellent agreement with the experimental results.

To obtain in the simulation this strong increase in bandwidth by coupling the PPR with the EPR, the emission wavelength has to be detuned away from the reflectivity peak, toward the long wavelength side; this is the so-called detuned loading regime [1]. By pushing the wavelength in the detuned loading regime, the differential gain increases and reduces the damping at higher frequencies.

An additional indication of the impact of the PPR to the high-frequency response can be observed in the emission spectrum, as plotted in Fig. 4. For static operation, one can see a featureless exponential decrease of the intensity nearby the emission wavelength. By high-frequency intensity modulation (0.5–20 GHz), additional side bands appear at a fixed frequency distance of about 42 GHz independently from the modulation frequency. This frequency splitting is in good agreement with the calculated PPR and confirms the coupling between EPR and PPR during modulation. We also have measured lasers with smaller cavities because our layout was limited to a laser length of 1.3 mm. These lasers show lesser high-frequency results like theoretical accepted because of the weaker coupling between the two resonances. An exact simulation for the other lengths were not possible due to the very high simulation complexity. A measurement of the sidebands of the other lasers were not accomplished.

The lasers also exhibit low noise figures. CW operating lasers show an RIN value per frequency unit of -144.2 dB/Hz, which should allow us to achieve low bit-error rates for high-speed optical transmission.

V. Conclusion

High-speed single-mode lasers were fabricated by FIB lithography based on laterally weakly coupled DBR gratings. The devices show stable emission characteristics, high single-mode output power, and improved directly modulated 3-dB bandwidth. SMSRs up to 48 dB were achieved with a grating length of 300 μm. From small signal response measurements, a 3-dB bandwidth of 22 GHz was obtained for a 1.3-mm-long device, which is 2.5 times larger in comparison to Fabry–Pérot lasers with the same cavity length. The improvement was achieved by utilizing the high-frequency PPR, which can be coupled to the EPR in the detuned loading regime by using weakly coupled gratings. To achieve the detuned loading regime, the detuning between the cavity mode and reflectivity peak has to be adjusted. This is either fixed by the device geometry or can be tuned by current injection in the grating section (not performed for the presented work). A better control of the operation conditions would be possible by using an additional phase-control section.

Acknowledgment

The authors would like to thank Alcatel Corporate Research Center, Opto+ for the supply of the laser structure, and A. Wolf for technical assistance during device processing.

References

[1] U. Feiste, "Optimization of modulation bandwidth in DBR lasers with detuned Bragg reflectors," *J. Quantum Electron.*, vol. 34, pp. 2371–2379, Dec. 1998.

[2] G. Morthier, R. Schatz, and O. Kjebon, "Extended modulation bandwidth of DBR and external cavity lasers by utilizing a cavity resonance for equalization," *IEEE J. Quantum Electron.*, vol. 36, pp. 1468–1475, Dec. 2000.

[3] K. Vahala and A. Yariv, "Detuned loading in coupled cavity semiconductor lasers-effect on quantum noise and dynamics," *Appl. Phys. Lett.*, vol. 45, no. 5, pp. 501–503, 1984.

[4] J. M. Verdiell, U. Koren, and T. L. Koch, "Linewidth an alpha-factor of detuned-loaded DBR lasers," *IEEE Photon. Technol. Lett.*, vol. 4, pp. 302–305, Apr. 1992.

[5] O. Kjebon, R. Schatz, S. Lourdudoss, S. Nilsson, B. Stålnacke, and L. Baeckbom, "30 GHz direct modulation bandwidth in detuned loaded InGaAsP DBR lasers at 1.55 μm," *Electron. Lett.*, vol. 33, no. 6, pp. 488–489, 1997.

[6] H. König, J. P. Reithmaier, and A. Forchel, "Highly resolved maskless patterning on InP by focused ion beam enhanced wet chemical etching," *Jpn. J. Appl. Phys.*, vol. 38, pp. 6142–6144, 1999.

[7] L. Bach, S. Rennon, J. P. Reithmaier, and A. Forchel, "Laterally coupled DBR laser emitting at 1.55 μm fabricated by focused ion beam lithography," *IEEE Photon. Technol. Lett.*, vol. 14, pp. 1037–1039, Aug. 2002.

[8] S. Rennon, L. Bach, J. P. Reithmaier, and A. Forchel, "Complex coupled distributed feedback and Bragg-reflector lasers for monolithic device integration based on focused-ion-beam technology," *IEEE J. Select. Topics Quantum Electron.*, vol. 7, pp. 306–311, Mar./Apr. 2001.

[9] T. Makino, "Transfer-matrix formulation of spontaneous emission noise of DFB semiconductor lasers," *J. Lightwave Technol.*, vol. 9, pp. 84–91, Jan. 1991.

[10] K. Byoung-Sung, C. Youngchul, and L. Jae-Seung, "An efficient split-step time-domain dynamic modeling of DFB/DBR laser diodes," *IEEE J. Quantum Electron.*, vol. 36, pp. 787–794, July 2000.